UNDERSTANDING THE PECULIARITIES OF ROTORCRAFT - PILOT - COUPLINGS

Marilena D. Pavel
Delft University of Technology
Delft, The Netherlands
m.d.pavel@tudelft.nl

Gareth D Padfield
The University of Liverpool
Liverpool, UK
gareth.padfield@liv.ac.uk

Rotorcraft pilots are familiar with potential instabilities or with annoying limit cycle oscillations that arise from the effort to control aircraft with high response bandwidth actuation systems. The destabilization of a vehicle due to active participation of the pilot in the control loop corresponds to the so-called '*rotorcraft-pilot coupling*' phenomenon (RPC). RPCs, in the past frequently called '*pilot induced/assisted oscillations*' (PIO/PAO), can be problematic for the safety of the aircraft. Generally, it is accepted that RPCs are much more difficult to predict and suppress than aircraft-pilot-couplings (APCs); APCs have been mainly associated with the lower frequency spectrum of the flight modes, while for modern helicopters RPCs can also be associated with the higher frequency spectrum of structural dynamic and rotor aeroelastic modes. The goal of the present paper is to present results of an analytic investigation to provide an improved understanding of the peculiar physical mechanisms through which the pilot excites the rotor regressive flap and lag modes in an RPC event, and how these modes can couple through the flight control system (FCS) to the airframe body roll mode. It will be demonstrated that for a hovering helicopter the FCS is primary responsible for transferring energy from the roll to the flapping motion but usually no energy is transferred back from the flapping to the roll motion. In the case of an RPC induced by a time delay between the pilot input and the aircraft response it appears that the time delay has not much influence on the limits of the attitude controller, however, there is energy transferred back from the flapping to the roll motion. The roll mode tends to couple primarily with the flapping motion which in turn couples with the lag motion and can contribute to the destabilizing flap-roll coupling in an RPC event. For the FCS or rotor system designer, the paper will derive stability criteria and boundaries for the roll attitude feedback/roll rate feedback gains for a hovering helicopter as a function of aircraft parameters.

Notation

C_l^{α} = lift slope [rad^{-1}]

C_{d0}, C_{d2} = profile drag coefficients $C_d = C_{d_0} + C_{d1}\alpha + C_{d2}\alpha^2$

g = gravity acceleration [m/sec^2]

h = height of main hub above helicopter centre of gravity (m)

I_{bl} = blade moment of inertia about flap/lag hinges (kg m^2)

I_x, I_y = helicopter moment of inertia about roll and pitch axes (kg m^2)

K_β K_ζ = flap and lag centre-spring rotor stiffness (Nm/rad)

K_ϕ = fuselage roll attitude gain (deg/deg)

K_p = fuselage roll rate gain (deg/deg/sec)

M_β = hub rolling moment per unit flapping $M_\beta = \frac{N}{2}K_\beta + T \cdot h$ (Nm/rad)

N = number of blades

p = helicopter roll rate (deg/sec)

q = helicopter pitch rate (deg/sec)

T = helicopter thrust [N]

v_i = inflow through the rotor disk (m/s)

α = rotor blade angle of attack

β_0, β_{1c}, β_{1s} = rotor blade coning, longitudinal and lateral flapping angles in multiblade coordinates

γ = Lock number $\gamma = \frac{\rho C_{l\alpha} c R^4}{I_{bl}}$

λ_β = non-dimensional flapping frequency $\lambda_\beta^2 = 1 + \frac{K_\beta}{I_\beta \Omega^2} = 1 + \nu_\beta^2$

λ_ζ, ν_ζ = non-dimensional lagging frequency $\lambda_\zeta^2 = \nu_\zeta^2 = \frac{K_\zeta}{I_{bl}\Omega^2}$

λ_i = non-dimensional inflow velocity $\lambda_i = \frac{v_i}{\Omega R}$

ν_β = non-dimensional rotating flapping frequency $\nu_\beta^2 = \frac{K_\beta}{I_\beta \Omega^2}$

ζ_0, ζ_{1c}, ζ_{1s} = rotor blade lag collective, longitudinal and lateral lag angles in multiblade coordinates

Presented at the American Helicopter Society 64nd Annual Forum, Montreal, Canada, April 29 – May 1, 2008.

ϕ = helicopter roll attitude angle

θ_{1s}, θ_{1c} = longitudinal and lateral cyclic pitch (θ_{1s} >0 for stick forward, θ_{1c} >0 for pilot stick to the left)

Ω = rotor rotational speed [rad/sec]

σ = blade solidity

τ = time delay between the pilot input and helicopter response [ms]

ψ = blade azimuth angle

Dressings

$\beta' = \frac{d\beta}{d\psi}$ = differentiation with respect to the azimuth angle

$\bar{p} = \frac{p}{\Omega}$ = roll rate normalized by the rotorspeed

Introduction

In the last decade there has been an increased and renewed interest in understanding the causes and remedies for so-called Aircraft and Rotorcraft Pilot Coupling (A/RPC) phenomena. A/RPCs are generally oscillations or divergent responses originating from adverse pilot-vehicle couplings. These undesirable couplings may result in potential instabilities or annoying limit cycle oscillations, degrading the aircraft handling qualities and risking exceedence of its structural strength envelope. The exceedence of structural strength limits can clearly result in catastrophic failures. In the aviation community A/RPCs are often known as Pilot Induced/Pilot Assisted oscillations (PIO/PAO).

According to ref. 12, Pilot Induced Oscillations (PIOs) occur when the pilot inadvertently causes divergent oscillations by applying control inputs that are essentially in the wrong direction or have a significant phase lag with respect to the aircraft response. Such oscillations can occur in configurations that are oversensitive to pilot inputs, or have excessively low natural frequencies and low response bandwidth. As a result '*angular acceleration responses are immediate and directly coupled to the stick inputs*' [ref. 1]. Since active involvement in the control loop is occurring, the pilot can stop the PIO by releasing the controls or changing his control strategy (for example reducing the closed loop gain).

Pilot Assisted Oscillations (PAOs) are the result of involuntary control inputs of the pilot in the loop that may destabilize the aircraft due to inadvertent couplings between the pilot and the aircraft. PAOs are actually high order PIOs, mostly associated with '*control system effects, including additional phase lags due to inappropriate filters and (to a limited extent) digital effect time delays, excessive command path gains, and actuation system saturation. The angular acceleration responses are lagged or delayed…"* (ref. 1). PAOs that involve passive involvement by the pilot's biodynamic response to vibration can be particularly dangerous because the action of releasing the controls may be dangerous in itself. Their essence is an oscillation at a frequency where the attitude response lags the stick inputs by approximately 180 degrees. Generally, both PIOs and PAOs are limit cycle type oscillations. In Ref. 12, McRuer recommended the use of the term A/RPC as a general term for this type of destabilization, considering PIOs and PAOs as subclasses of A/RPCs (ref. 12). McRuer classified A/RPCs in three categories:

- Cat. I assumes linear behavior of the pilot and control system. The oscillations are associated with high gains and increased time delay effects, typically resulting in a destabilization of the closed loop pilot-vehicle system.
- Cat. II involves limit cycle oscillations of the pilot-vehicle system due to nonlinear control elements in the feedback system (such as rate and position limiters).
- Cat. III covers severe pilot-vehicle oscillations, which are inherently non-linear and characterized by a transition from one transient response to another.

Reference 10 suggested introducing a Category IV A/RPC for events that are caused by, or have as a major contributor, structural modes and their interactions with the pilot. This category may be of particular interest for the rotorcraft [ref. 17].

Aircraft-and-rotorcraft-pilot couplings are an important impediment to the design of modern configurations. The problem is that the rapid advances in the field of flight control systems (FCSs) seems to have contributed to a process of pilot desensitization, i.e. "cutting-off" the physical connection between the pilot and the aircraft and masking the vehicle's approach to the limits of control. For APC, this process is explained as follows: "*The primary function of flight control laws is to provide the aircraft with good handling qualities by using feedback of the 'rigid aircraft' motion to the flying control surfaces. However, the airframe is not anymore rigid and has many structural modes of vibration that will be excited by the control surface movements*. *The response of these lightly damped modes is usually detected by the motion sensors and fed back to the control surfaces, with the potential for closed-loop instability at the structural mode frequencies*" [ref. 1]. For rotorcraft, this situation is even more complicated. In the next paragraph some typical rotorcraft

peculiarities that enhance the development of adverse RPC will be discussed. Quoting from one recent research investigation, "*More rather than fewer severe PIOs are likely to be introduced in the future unless something will change*" [ref. 11]. Clearly there is a real need for better design guidance here.

Peculiarities of RPCs

Rotorcraft-pilot-couplings are, generally speaking, much more complicated to understand than aircraft-pilot-couplings (ref. 6). The primary reason for this is that rotorcraft possess characteristics resulting from the interactions between the rotating system - the rotor, and the fixed system - the airframe. Reference 16 gives a good background for understanding the peculiar behavior of rotorcraft with a pilot in the loop.

In conventional fixed-wing aircraft, control moments are transmitted directly from the control surfaces to the aircraft. In contrast, with helicopters, the control inputs are transmitted through the swash plate to the blade pitch, causing the rotor to flap and thence transmitting moments to the aircraft. It is well-known that cyclic inputs are applied at 1/rev-frequency through this swash plate mechanism. Thus, low-frequency pilot inputs generate high-frequency blade excitations. Clearly, rotor blade excitations, in the form of flap and lag motion, can be transformed back to the fixed airframe system, where eventually a new 1/rev-frequency shift may occur with positive or negative sign. In order to comprehend this transformation mechanism of multi-bladed rotor systems, the concept of rotor modes is helpful:

- Collective rotor mode dynamics are transferred directly without frequency shift.
- Cyclic rotor mode dynamics (so - called progressive and regressive modes) are transformed with a ±1/rev frequency shift.

This short explanation of the airframe-rotor-airframe transformation behavior characteristic to helicopters is of fundamental importance for understanding rotorcraft RPCs.

Furthermore, RPCs are more complicated to understand because the airframe-rotor-airframe interaction differs for an articulated and a hingeless helicopter. *'The dynamics of the fuselage and the rotor of an articulated helicopter can usually be seen as a 'cascade problem', i.e. a rapid rotor plane response followed by a slower fuselage response. For hingeless rotor configurations, the body motion 'speeds up' and the rotor dynamics enter into the body dynamics'* (ref. 3).

Based on flight experience with modern helicopters, it appears that RPCs of special interest are associated mainly with the high-frequency spectrum of structural dynamic and aeroelastic modes (refs. 1, 5, 16, 17). Well-known examples of helicopter RPCs have been related to:

- excitation of the low - damped main rotor regressive-inplane mode by cyclic inputs resulting in aircraft roll and pitch vibrations;
- excitation of the low frequency pendulum mode of external slung loads by delayed collective and/or cyclic control inputs due to couplings of the load dynamics via elastic cables.

The physical mechanism through which the pilot excites the rotor cyclic/collective modes in a RPC is presently not fully understood. It is the goal of this paper to contribute to understanding the physical mechanism through which the pilot excites the rotor higher-order dynamics in a RPC event.

Helicopter roll subsidence – regressing flap mode coupling through the control system

As a first example, the paper will concentrate on the mechanism through which cyclic pitch can excite the rotor regressive-flap mode, and how this coupling can induce unstable body pitch/roll motions. It is of course well known that the dynamics of the fuselage can couple with the dynamics of the rotor. Curtiss (refs. 3, 4) showed that for an articulated rotor the body roll mode in particular tends to combine with the flapping regressing mode and impose limitations on the attitude feedback gain of an automatic flight control system (FCS). High gain attitude control is therefore seen to present a problem for pilots and FCS designers. We can obtain some insight into the loss of damping in the roll/flap regressive mode through an approximate stability analysis of the coupled system at the point of instability. The following assumptions are made: 1) the first-order linear representation of multi-blade flapping dynamics is adequate for predicting the behavior of the regressing flap mode; 2) the low modulus fuselage dynamics is neglected.

In Reference 14 (pp. 286) the equations of motion for the coupled rotor flap-fuselage angular motion in hover are derived as an approximate 4^{th} order linear coupled system of equations in $\{\beta_{1s}, \beta_{1c}, q, p\}$:

$$\begin{bmatrix} -2 & \gamma/8 \\ \gamma/8 & 2 \end{bmatrix}\begin{bmatrix} \beta_{1c}' \\ \beta_{1s}' \end{bmatrix} - \begin{bmatrix} \gamma/8 & -\left(\lambda_\beta{}^2 - 1\right) \\ -\left(\lambda_\beta{}^2 - 1\right) & -\gamma/8 \end{bmatrix} \times$$
$$\begin{bmatrix} \beta_{1c} \\ \beta_{1s} \end{bmatrix} == \begin{bmatrix} -2\overline{q} + \left(\theta_{1s} + \overline{p}\right)\gamma/8 \\ 2\overline{p} + \left(\theta_{1c} + \overline{q}\right)\gamma/8 \end{bmatrix} \qquad (1)$$
$$I_y \overline{q}' = -\frac{M_\beta}{\Omega^2}\beta_{1c}$$
$$I_x \overline{p}' = -\frac{M_\beta}{\Omega^2}\beta_{1s}$$

where β_{1s} and β_{1c} represent the lateral disc tilt and the longitudinal disc tilt respectively; p and q are the fuselage roll rate and pitch rate respectively. The prime ' in the system of equations (1), denotes differentiation w.r.t. azimuth angle ψ, e.g. $\beta_{1c}' = d\beta_{1c}/d\psi$; p and q are normalized by the rotorspeed, e.g. $\overline{p} = p/\Omega; \overline{q} = q/\Omega$.

$M_\beta = \frac{N}{2}K_\beta + T \cdot h$ represents the moment exerted on the body per radian of rotor disc-tilt, due to the rotor thrust vector T, offset w.r.t. the body center of gravity, as well as due to direct hub centre-spring rotor stiffness K_β (see Figure 1).

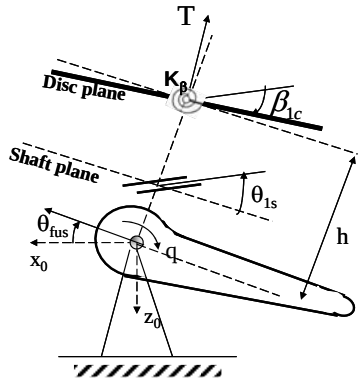

Figure 1: *Explanation of M_β term*

It is assumed that the pilot can control the helicopter roll attitude ϕ with the lateral cyclic pitch θ_{1c} using a proportional-derivative (PD) controller in the form:

$$\theta_{1c}(t) = K_\phi \phi(t) + K_p\, p(t), \quad K_\phi > 0; K_p > 0 \qquad (2)$$

where K_ϕ and K_p are the roll attitude feedback gain and roll rate feedback gain respectively. Substituting (2) into (1) and writing the system in matrix form leads to a 5th order system of equations in {β_{1s}, β_{1c}, q, p, ϕ}, see eq. (A4). For high values of feedback gain one can make the assumption that the regressing flap mode couples with the roll subsidence mode to define a high modulus system, so that the pitch motion q decouples from the system. A 4th order system of equations in {β_{1s}, β_{1c}, p, ϕ} is then obtained, see eq. (A7), characterizing the coupled roll-flap regressing system (see Appendix A for a complete derivation of the system in matrix form):

$$\begin{bmatrix} \beta_{1c}' \\ \beta_{1s}' \\ \overline{p}' \\ \phi' \end{bmatrix} = A_{RF}^{**}\begin{bmatrix} \beta_{1c} \\ \beta_{1s} \\ \overline{p} \\ \phi \end{bmatrix} + B_{RF}^{**}\theta_{1s} \qquad (3)$$

with roll-flap matrices A_{RF} and B_{RF} given by (A8) and (A9).

In order to understand how the main rotor regressive flap mode can be excited by pilot or FCS cyclic control inputs, expressions for the frequency and damping of the coupled flap-roll modes can be examined as given by (3). As case applications the paper considers three different helicopters - Puma, Lynx and Bo-105 differing through their rotor system and overall size and mass. The configuration parameters used for the numerical simulations are summarized in Table 1 (ref. 14).

Table 1: Configuration data

Parameters	Bo-105	Puma	Lynx
γ (–)	5	9.374	7.12
I_x (kg m^2)	1803	9638	2767
Ω (rad/s)	44.4	28.3	35.63
K_β (Nm/rad)	113330	48149	166352
I_{bl} (kg m^2)	231.7	1280	678.14
M (kg)	2200	5805	4313.7
h (m)	0.944	1.875	1.274
Nb. Blades N (-)	4	4	4
$M_\beta = \frac{N}{2}K_\beta + M \cdot g \cdot h$ (N m)	247048	106776	386616
$\lambda_\beta = \sqrt{1 + \frac{K_\beta}{I_{bl}\Omega^2}}$ (-)	1.12	1.02	1.092

Figure 2 represents the position of the coupled regressing flap - roll pole $s_{\beta\zeta}$ and roll-regressing flap pole $s_{\zeta\beta}$ for the Bo105 configuration (these poles mean that the motion is assumed coupled, the flap-roll pole being dominated by flapping and the roll-flap pole being dominated by the roll motion).

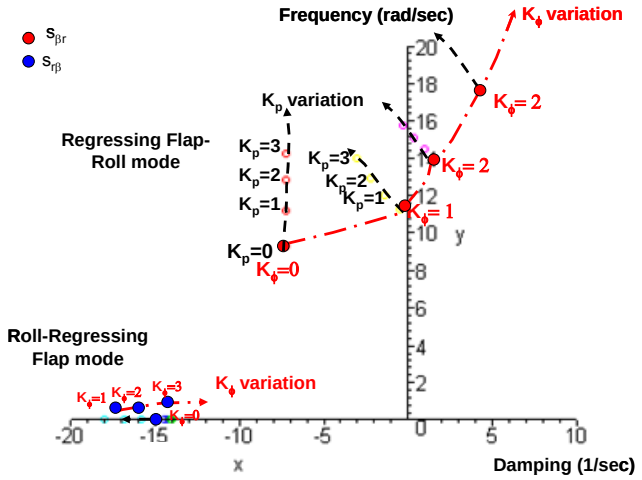

Figure 2: *Root loci for varying roll attitude and roll rate feedback gains for Bo-105 in hover, body-flap motion*

It can be seen that the most direct way for destabilizing these modes lies in the variation of the K_ϕ and K_p gains. From Figure 2, it appears that varying the roll attitude feedback gain destabilizes the flap-roll motion, decreasing the damping of the flap-roll mode and increasing its frequency. From a gain K_ϕ=1 (deg/deg) onward the motion becomes unstable and the damping in the roll-flap mode decreases very rapidly. Varying the roll rate feedback gain K_p results actually in stabilizing the motion as shown in Figure 2. Thus, varying the attitude gain feedback results primarily in coupling the body to flap motion. This result can be found also in the literature [example ref. 3, ref 14 pp 287].

Returning to the roll-regressing flap motion given by eqs. (3), some insight can be gained into the loss of damping in the roll-flap regressing mode through an approximate stability analysis of the coupled system at the point of instability. The characteristic equation of the 4th order roll-flap system of equations (3) has the form:

$$a_4\lambda^4 + a_3\lambda^3 + a_2\lambda^2 + a_1\lambda + a_0 = 0 \qquad (4)$$

where the coefficients a_4, a_3, a_2, a_1 and a_0 are given in (A11). The condition for stability of the coupled flap-lag mode is given by the Routh-Hurwitz criterion [ref. 2]. Assuming a_4>0 (which is true as a_4=1) one obtains the stability conditions as:

$$a_3 a_2 - a_1 a_4 > 0 \qquad (5)$$

$$a_1\left(a_3 a_2 - a_1 a_4\right) - a_3^{\,2} a_0 > 0 \qquad (6)$$

$$a_3 > 0; \quad a_0 > 0 \qquad (7)$$

From the expressions for a_3 and a_0 given by (A11) it follows that condition (7) is always fulfilled. Condition (5) leads to the following stability criterion in terms of the roll attitude feedback gain:

when applying a controller $\theta_{1c} = K_\phi\phi, \quad K_\phi > 0$

$$K_\phi < \left(1+\lambda_\beta^{\,2}\right)\left\{\frac{\Omega^2\left[\frac{\gamma^2}{64}+\left(\lambda_\beta^{\,2}-1\right)^2\right]}{\frac{M_\beta}{I_x}\left[\frac{1}{16}+\left(\frac{\gamma}{64}\right)^2\right]}+\frac{1}{2}\right\} \qquad (8)$$

A value K_ϕ higher than that given in equation (8) will drive the fuselage flap-mode unstable.

when using a controller

$$\theta_{1c} = K_\phi\phi + K_p p, \quad K_\phi > 0; K_p > 0$$

$$K_\phi < \left(1+\lambda_\beta^{\,2}\right)\left\{\frac{\Omega^2\left[\frac{\gamma^2}{64}+\left(\lambda_\beta^{\,2}-1\right)^2\right]}{\frac{M_\beta}{I_x}\left[\frac{1}{16}+\left(\frac{\gamma}{64}\right)^2\right]}+\frac{1}{2}\right\}+ \qquad (9)$$

$$\frac{\gamma}{16}\frac{\lambda_\beta^{\,2}-\frac{1}{4}\cdot\frac{\gamma^2}{64}}{1+\frac{1}{4}\cdot\frac{\gamma^2}{64}}K_p$$

In criterion (9) there are four parameters of importance which can excite the rotor flapping motion:

1) $M_\beta / I_x = \omega_\phi^2$ representing the 'natural' frequency of the pure roll motion when assuming small roll and lateral flapping angles (including constant rotor thrust), see (ref. 14, pp. 311);

2) λ_β the flap frequency ratio $\lambda_\beta^2 = 1+\frac{K_\beta}{I_\beta\Omega^2} = 1+\nu_\beta^2$;

3) Ω the rotorspeed;

4) γ the Lock number.

The most critical parameters are the rotorspeed and hub stiffness K_β; slow, stiff rotors being the most susceptible to the excitation of the flap regressing mode by cyclic pitch inputs.

Helicopter roll subsidence - regressing flap - regressing lag modes coupling through the control system

The next question is then how can the main rotor in-plane motion be excited by cyclic control inputs? The equations of motion for the coupled rotor flap-lag-fuselage angular motions in hover can be derived using, e.g., Lagrange's method (assuming that the flap and lag hinge coincide). After linearizing the system, a 6th order linear coupled system of equations in $\{\beta_{1c}, \beta_{1s}, \zeta_{1c}, \zeta_{1s}, q, p\}$ is obtained,:

$$\begin{bmatrix} -2 & \gamma/8 & 0 & 2\beta_0 \\ \gamma/8 & 2 & -2\beta_0 & 0 \\ 0 & -2\beta_0 & -2 & -\gamma C_{d_2} C_l^\alpha \\ 2\beta_0 & 0 & -\gamma C_{d2} C_l^\alpha & 0 \end{bmatrix} \begin{bmatrix} \beta_{1c}' \\ \beta_{1s}' \\ \varsigma_{1c}' \\ \varsigma_{1s}' \end{bmatrix} -$$

$$\begin{bmatrix} \gamma/8 & -\left(\lambda_\beta^{\,2}-1\right) & -2\beta_0 & 0 \\ -\left(\lambda_\beta^{\,2}-1\right) & -\gamma/8 & 0 & 2\beta_0 \\ 2\beta_0 & -(\gamma/4)\beta_0 \dfrac{C_{d_0}}{C_l^\alpha} & (\gamma/4)\dfrac{C_{d_0}}{C_l^\alpha} & -\left(\lambda_\varsigma^{\,2}+1\right) \\ -(\gamma/4)\beta_0 \dfrac{C_{d_0}}{C_l^\alpha} & -2\beta_0 & -\left(\lambda_\varsigma^{\,2}+1\right) & -(\gamma/4)\dfrac{C_{d_0}}{C_l^\alpha} \end{bmatrix} \times$$

$$\begin{bmatrix} \beta_{1c} \\ \beta_{1s} \\ \varsigma_{1c} \\ \varsigma_{1s} \end{bmatrix} = \begin{bmatrix} -2\bar{q} + 2\bar{p}\varsigma_0 + \left(\theta_{1s} + \bar{q}\varsigma_0 + \bar{p}\right)\gamma/8 \\ 2\bar{p} + 2\bar{q}\varsigma_0 + \left(\theta_{1c} + \bar{p}\varsigma_0 + \bar{q}\right)\gamma/8 \\ 0 \\ 0 \end{bmatrix}$$

$$I_y \bar{q}' = -\frac{M_\beta}{\Omega^2}\beta_{1c}$$

$$I_x \bar{p}' = -\frac{M_\beta}{\Omega^2}\beta_{1s} \qquad (10)$$

where β_0 and ζ_0 are the steady-state values of flap β and lag ζ. $\lambda_\varsigma^2 = \dfrac{K_\varsigma}{I_{bl}\Omega^2}$ is the non-dimensional lead-lag frequency and C_{d_0}, C_{d2} the blade profile drag coefficients $C_d = C_{d_0} + C_{d1}\alpha + C_{d2}\alpha^2$.

With the pilot controlling the roll motion ϕ with lateral cyclic pitch θ_{1c} using a PD controller, as given in eq. (2) and substituting this into (10), leads to a 7th order system of equations in $\{\beta_{1s}, \beta_{1c}, \zeta_{1c}, \zeta_{1s}, q, p, \phi\}$. Assuming that, for high values of feedback gain, the flap-lag mode couples with the roll subsidence mode to define a high modulus system, a 6th order system of equations in $\{\beta_{1s}, \beta_{1c}, \zeta_{1c}, \zeta_{1s}, p, \phi\}$ is obtained.

An understanding of how the rotor in-plane motion is excited by cyclic pitch, can be gained by examining the frequency and damping of the coupled flap-lag-roll motion. Figure 3 represents the flap-lag $s_{\beta\zeta}$ and lag-flap $s_{\zeta\beta}$ poles, again for the Bo105 configuration.

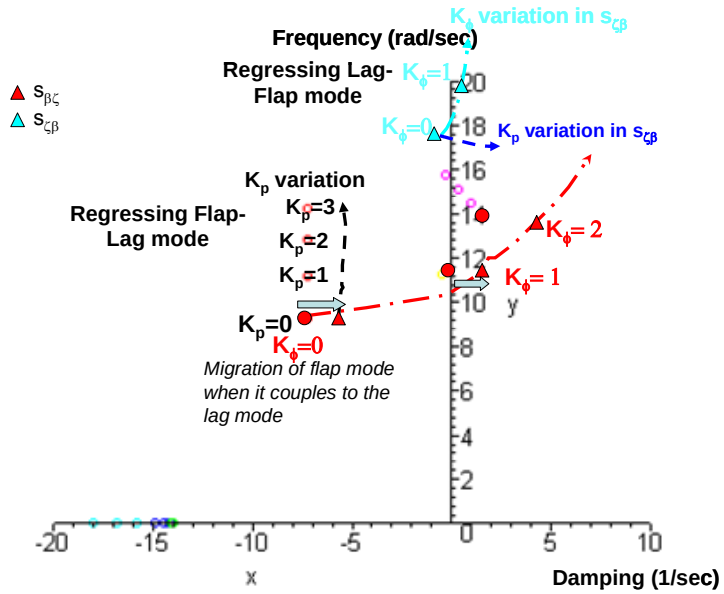

Figure 3 *Root loci for varying roll attitude and roll rate feedback gains for Bo-105 in hover, body-flap-lag motion*

From Fig 3 it can be seen that the damping of the new flap-lag mode decreases and the roll rate feedback gain destabilizes the low-damping regressive in-plane motion. According to ref. 5, air resonance can be expected whenever the frequency of the coupled roll-flap mode is in close proximity to the frequency of the roll-regressing lag mode. The rate gain K_p is primarily responsible for destabilizing the flap-lag mode and bringing closer the roll-flap and roll-in-plane modes. Thus, the rate gain is limited primarily by the lag-body coupling. This result was also given in ref. 3.

As in the previous paragraph, an approximate stability analysis of the coupled system (10) at the point of instability can be carried out. Figure 4 presents the stability limits as a function of roll feedback gains for three different helicopters - Puma, Lynx and Bo-105 differing through their rotor system and overall size and mass.

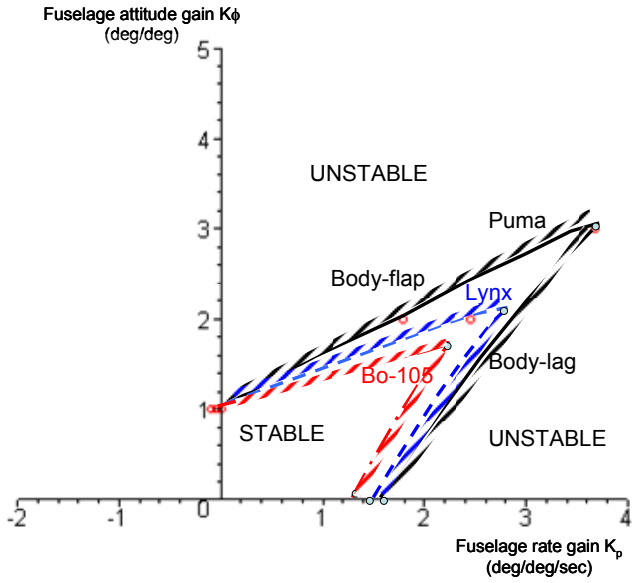

Figure 4: *Stability boundaries for roll attitude feedback gain- roll rate feedback gain, hovering helicopter*

One can see that the smallest stable region corresponds to the Bo-105. This is a soft flapwise, soft inplane rotor with a stiff flapwise hub [ref. 7]. [1] Lynx hingeless rotor design corresponds to a soft flapwise, soft inplane rotor with a soft flapwise hub (the motivation of Lynx soft hub in the soft inplane rotor was the need for an effectively matched stiffness design). On the Puma, with its slower turning, articulated rotor with higher Lock number, the allowable gain range is quite high (about 3 deg/deg). '*For the Lynx, the relatively high value of hub stiffness reduces the allowable level of feedback gain, but conversely, the relatively high rotorspeed on the Lynx serves to increase the usable range of feedback gain. Slow, stiff rotors would clearly be the most susceptible to the destabilizing effect of roll attitude to lateral cyclic feedback gain*' [ref. 14].

[1] Hingeless rotors can be classified as either soft or stiff depending on the fundamental blade flap and lag frequency. Using as a parameter the blade flapping frequency, Hohemenser [ref. 7] introduced the concept of soft-flapwise rotor when the fundamental flap frequency was 1.05 to 1.15/rev and stiff-flapwise rotor if this frequency was 1.4/rev or more. Using as parameter the blade lead-lag natural frequency, the rotor can be soft-inplane when the blade natural frequency is smaller than 1/rev and stiff-inplane if this frequency is larger than 1/rev. Articulated rotors correspond usually to soft-flapwise, soft-inplane configurations.

The Mechanism of flap-lag-roll coupling

The mechanism through which the higher-order flap-lag rotor dynamics couples with the body dynamics can be understood better by applying the so-called "energy-flow method", a semi-qualitative method for identifying the mechanism of a dynamic instability [ref. 12]. The idea of this method is that any instability possesses a multiplicity of energy flow paths (vicious circles) in which energy is transferred from one degree of freedom to the other. The method follows the steps:

1) The dynamical equations of motion are written as a set of second-order systems;
2) Each degree of freedom (DOF) is considered as an excitation for the other DOF => the coupling terms are external excitations for each separate degree of freedom;
3) It is assumed that there is "virtual" damping in each degree of freedom such that an oscillation with constant amplitude results. The amount of damping does not depend on the actual damping;
4) Next, one inspects whether there are any external excitations (coupling terms) in phase with the velocity of the degree of freedom considered. If so, the coupling term - "excitation" - pumps energy into or extracts energy from the DOF.
5) If there are degrees of freedom which mutually pump energy into each other, this indicates the possibility of dynamic instability. The reasoning here is that the added virtual damping must continuously dissipate energy to achieve the constant amplitude. If the actual damping is less, then the mutual energy exchange would tend to increase the motion amplitude.

The energy flow method can be applied to the flap-lag-roll motion to obtain a physical understanding and feeling for the energy flow interchanged between the body roll and rotor flap-lag dynamics. Equation (10) can be re-written in the *rotating system of reference* with the coupling terms as excitation forces on the right-hand side of the equation, as follows:

Flap equation:

$$\underset{iner.}{\beta''} + \underset{aerodyn}{\frac{\gamma}{8}\beta'} + \underset{cf.+elastic\ spring}{\left(1+\nu_\beta^{\,2}\right)\beta} = \underset{Coriolis}{-2\beta_0\nu_\beta^{\,2}\varsigma'} \underset{Coriolis}{+2\bar{p}\cos\psi} \underset{aerodyn.term}{+\frac{\gamma}{8}\theta_{1c}\cos\psi} \underset{aerodyn.term}{-\frac{\gamma}{8}\bar{p}\sin\psi} = M_\beta \qquad (11)$$

Lag equation:

$$\underset{iner.}{\varsigma''} + \underset{elastic\ spring}{\nu_\varsigma^{\,2}\varsigma} = \underset{Coriolis}{-\left(\nu_\beta^{\,2}-1\right)\beta_0\beta'} \underset{aerodyn.term}{+\frac{\gamma}{3}\bar{p}\lambda_i\sin\psi} \underset{aerodyn.term}{+\frac{\gamma}{6}\bar{p}\lambda_i\theta_{1c}\cos\psi} = M_\varsigma \qquad (12)$$

Roll subsidence equation:

$$\phi'' = -\frac{M_\beta}{\Omega^2 I_x}\frac{2}{3}\sum_{k=1}^{N}\beta_k \sin\psi_k = M_\phi \qquad (13)$$

Assume that all the natural frequencies are close to each other, i.e.:

$$1+\nu_\beta^{\,2} \approx \nu_\varsigma^{\,2} \approx \nu^2 \qquad (14)$$

Consider first that the roll motion is an "external" excitation for the flapping system. Assume also that the resulting flapping motion is a constant amplitude oscillation varying as $\cos\nu\psi$, i.e. $\beta \propto \cos\nu\psi$ (β proportional to $\cos\nu\psi$). The flap velocity is then proportional to $\beta' \propto -\sin\nu\psi$. The excitation M_ϕ of the roll motion then takes the form

$$M_\phi \propto -\frac{M_\beta}{\Omega^2 I_x}\frac{2}{3}\cos\nu\psi\sin\psi \propto -\frac{M_\beta}{\Omega^2 I_x}\frac{1}{3}\left[\begin{matrix}\sin(1+\nu)\psi + \\ \sin\left((1-\nu)\psi\right.\end{matrix}\right] \qquad (15)$$

The response of the roll motion is then, from eq.(12), proportional to:

$$\phi \propto \frac{1}{(1+\nu)^2}\sin((1+\nu)\psi + \frac{1}{(1-\nu)^2}\sin((1-\nu)\psi \qquad (16)$$

It is known that the cause of any instability can be found in the fact that any unstable system has destabilizing forces – so-called "drivers" acting on a specific degree of freedom of the system which have components in phase with the velocity of the corresponding degree of freedom. These forces produce work on the system, so they pump energy into the degree of freedom, [ref. 2]. For our case this would be true if the excitation M_ϕ which represents the coupling roll-flap term is in phase with the system's roll velocity. From Figure 2 and Figure 3 it can be seen that this happens when the lateral cyclic inputs are given by a controller of gain $K_\phi \neq 0$. In this case, eq. (13) would give a natural frequency $\nu_\phi^{\,2}$ and, assuming that $\nu_\phi^{\,2} = \nu^2$, it follows that the frequency of the excitation force M_ϕ is the same as the natural roll frequency of the system, so the system is at resonance. It is known that in a resonant system, the phase angle between the excitation and the resulting motion is always 90 deg, irrespective of the amount of damping that exists in the system. This means that the system's maximum response comes 90 deg after the maximum excitation is applied, i.e.:

$$\phi \propto \frac{1}{(1+\nu)^2}\sin((1+\nu+90)\psi + \frac{1}{(1-\nu)^2}\sin\left(\begin{matrix}1-\nu \\ +90\end{matrix}\right)\psi = \frac{1}{(1+\nu)^2}\cos((1+\nu)\psi + \frac{1}{(1-\nu)^2}\cos((1-\nu)\psi \qquad (17)$$

The roll attitude velocity,

$$\phi' \propto -\frac{1}{(1+\nu)}\sin(1+\nu)\psi - \frac{1}{(1-\nu)}\sin((1-\nu)\psi\,,$$

and contains terms in phase with the excitation M_ϕ. It follows that the flap motion pumps energy into the roll motion when a controller is introduced in the system with gain $K_\phi \neq 0$.

Consider next that the flapping motion acts as an external excitation for the roll motion. The response of the roll motion (17) causes, in turn, an external excitation of the flapping motion (see eq. (11)):

$$M_\beta \propto 2\phi'\cos\psi + \frac{\gamma}{8}(K_\phi\phi + K_p\phi')\cos\psi - \frac{\gamma}{8}\phi'\sin\psi = \frac{\sin\nu\psi}{(\nu+1)^2(\nu-1)^2}\left[\begin{matrix}\left(2+\frac{\gamma}{8}K_p\right)\nu\left(\nu^2-1\right)\left(1+\cos 2\psi\right)+ \\ \frac{\gamma}{8}\left(\nu\left(\nu^2-1\right)+K_\phi\left(\nu^2+1\right)\right)\sin 2\psi\end{matrix}\right] + \frac{\cos\nu\psi}{(\nu+1)^2(\nu-1)^2}\left[\begin{matrix}\left(2+\frac{\gamma}{8}K_p\right)\left(\nu^2-1\right)\sin 2\psi + \\ \frac{\gamma}{8}\left(\nu^2-1\right)\left(-1+\cos 2\psi\right)+\frac{\gamma}{8}K_\phi\cdot \\ \left(\nu^2+1\right)\left(1+\cos 2\psi\right)\end{matrix}\right] \qquad (18)$$

Comparing eq. (18) to the flapping velocity $\beta' \propto -\sin\nu\psi$, it follows that energy flow is transmitted from the roll to the flapping motion when M_β contains terms proportional with the flap velocity. This means that the term in $\sin\nu\psi$ in eq. (18) must satisfy the following condition:

$$\frac{1}{(\nu+1)^2(\nu-1)^2}\left[\begin{matrix}\left(2+\frac{\gamma}{8}K_p\right)\nu\left(\nu^2-1\right)\left(1+\cos 2\psi\right)+ \\ \frac{\gamma}{8}\left(\nu\left(\nu^2-1\right)+K_\phi\left(\nu^2+1\right)\right)\sin 2\psi\end{matrix}\right] < 0 \qquad (19)$$

Rearranging the terms in the parenthesis of eq. (17) and identifying the sign of each term gives the condition:

$$\underbrace{\frac{\gamma}{8}K_\phi\left(\nu^2+1\right)\underbrace{\sin 2\psi}_{+/-\,fct(\psi)}}_{+}+\underbrace{\frac{\gamma}{8}K_p\left(\nu^2-1\right)}_{+}\underbrace{\left(1+\cos 2\psi\right)}_{+}+$$
$$\underbrace{2\nu\left(\nu^2-1\right)+2\nu\left(\nu^2-1\right)\cos 2\psi+\frac{\gamma}{8}\nu\left(\nu^2-1\right)\sin 2\psi}_{+\ for\ \gamma\in[5,15]}>0 \qquad (20)$$

As it is assumed that $1+\nu_\beta{}^2\approx\nu_\varsigma{}^2\approx\nu^2>1$ (see eq. (14)), it follows that the sign of (20) is positive and opposite to the flapping velocity $\beta'\propto-\sin\nu\psi$, so no energy is transmitted from the roll to the flapping motion in normal operation conditions.

Figure 5 summarizes the energy-flow mechanism through which the flap and roll modes transfer energy into each other.

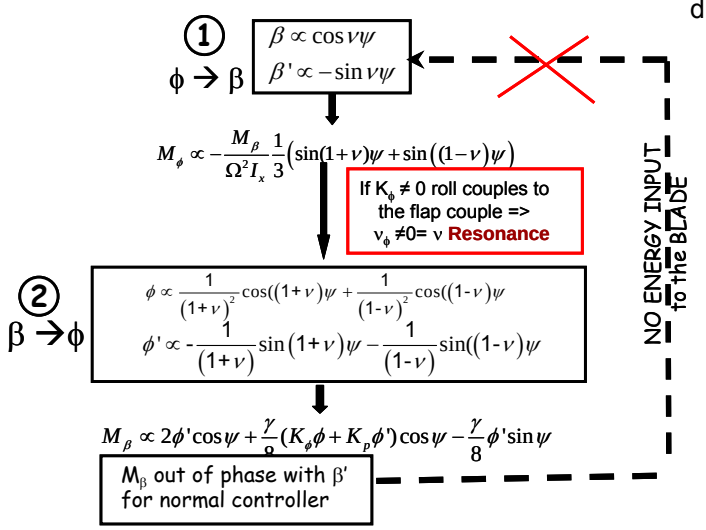

Figure 5: *The mechanism of roll-flap coupling in the energy flow method*

Returning to the flap-lag-roll equations of motion, (11) to (13), the next step is to investigate the influence of the lag motion on the flap-roll coupling. Appendix B presents the energy flow method in the case of flap-lag motion in the rotating frame (see also [ref. 15]). It is concluded that the flap-lag coupling is the strongest if the non-dimensional rotating flapping frequency lies in the range $1<\lambda_\beta<1.15$ and $\lambda_\varsigma>1$ (according to ref. 7 this corresponds to a soft-flapwise, stiff-inplane rotor). Physically, in a soft-flapwise rotor, the regressing flapping corresponds to a disc plane tilting in the same direction as the rotor rotation. In a stiff-inplane rotor, the regressing lag mode corresponds to a whirling of the rotor centre of mass opposite to the rotor rotation. Appendix B shows that also that the most critical parameter allowing transfer of energy from lag to flap is the term $(\nu_\beta^2-1)\beta_0\beta'$ and represents the Coriolis force on the blade due to a flapping velocity. This agrees with the classical theory on flap-lag instability, see e.g. ref. 9.

For the flap-lag-roll coupling mechanism, eq. (12) and (13) shows that the roll can excite the lag but the lag cannot excite the roll as eq. (13) does not contain lag 'excitation' terms. Therefore, the lag motion does not couple directly with the roll motion but, instead, it pumps energy through the flap motion.

To summarize the discussion of the roll-flap-lag mechanism, Figure 6 plots the paths through which vicious circles of energy transfer are formed between the flap-lag-roll degrees of freedom. The following conclusions on the roll-flap-lag mechanism can be drawn:

1) when using a controller, the roll motion pumps energy into the flap but the energy flow is usually not closed (no instability problem except when condition (9) is not fulfilled);
2) the flap-lag motions pump energy into each other especially in a soft-flapwise stiff-inplane rotor;
3) although the roll-lag motions are not directly related (the roll can pump energy into the lag but not the other way around), from Figure 4 it appears that it is possible for the fuselage-lag mode to be driven unstable for a certain value of roll rate gain. In this case, ϕ drives the lag motion unstable, the lag drives the flap unstable and, as a result, a closed-loop energy flow appears between β–ζ–ϕ as shown in Figure 6 (green and red lines).

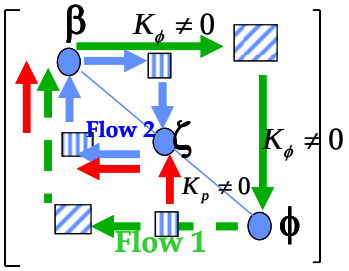

Figure 6: *The energy flow in the roll-flap-lag dynamic system*

Reference 14 comments on the way a controller can contribute to an unstable closed loop, noting that '*the presence of the rotor and other higher-order dynamic elements introduces a lag between the pilot and the aircraft's response to controls. The pilot introduces an even further delay through neuro-muscular effects and the combination of the two effects … can lead to a*

deterioration in the pilot's perception of aircraft handling' and finally to a PAO event. In the next section the contribution of pilot (or control system) time delays to the coupled pilot-vehicle dynamics will be investigated.

The mechanism of roll - flap - lag coupling in a Category I RPC

A key design concern relates to the limits on attitude and rate gains before the fuselage-flap motions are driven unstable in a RPC event. Consider a Category I event which is commonly induced by a time delay in the system. Figure 7 illustrates the sequence of pilot's control corrective movements and vehicle-body reaction in a RPC event (the angles have been exaggerated for emphasis). One can see that in RPC the pilot has a delayed control to vehicle-body reaction, controlling in the same direction as the body motion ($\theta_{1c} < 0$ while $\dot{\phi}_f > 0$)

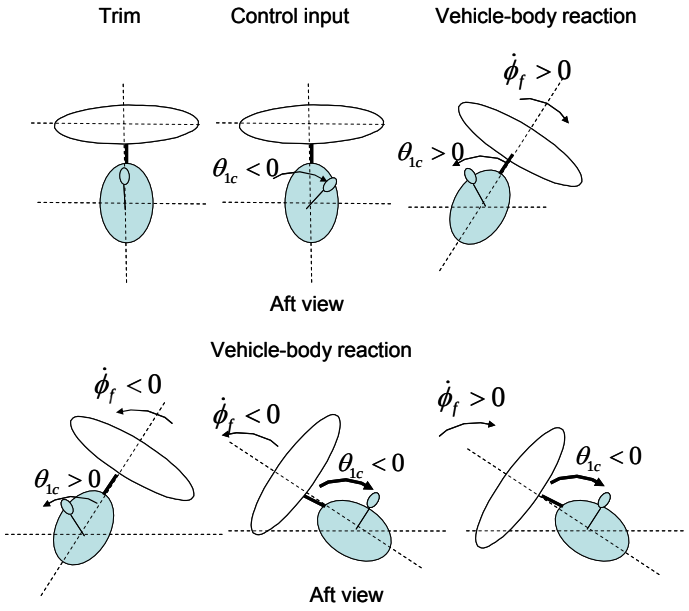

Figure 7: *Explaining the PIO as a lagging pilot control*

The delayed pilot lateral cyclic input can be approximated in a Taylor series in the form:

$$\theta_{1c}(t-\tau) = K_\phi \phi(t-\tau) \approx$$
$$K_\phi \left[\phi(t) + \frac{\dot{\phi}(t)}{1!}(t-\tau-t) + \frac{\ddot{\phi}(t)}{2!}(t-\tau-t)^2 \right] = \quad (21)$$
$$K_\phi \phi - K_\phi \tau \dot{\phi} + \frac{\tau^2}{2} K_\phi \ddot{\phi} = K_\phi \phi - K_\phi \tau p + \frac{\tau^2}{2} K_\phi \dot{p}$$

Rewriting condition (5) for the stability of the coupled flap-lag motion and neglecting the 2nd order term in the Taylor series (representing the roll acceleration feedback gain), the condition for stability in terms of the roll attitude feedback gain in a category I RPC event for the helicopter in hover can be written as (cf. equation (8)):

$$K_\phi < \frac{\left(1+\lambda_\beta^2\right)\left\{ \frac{\Omega^2\left[\gamma^2/64 + \left(\lambda_\beta^2 - 1\right)^2\right]}{\frac{M_\beta}{I_{xx}}\left[1/16 + \left(\gamma/64\right)^2\right]} + \frac{1}{2} \right\}}{1 + \frac{\gamma}{16}\frac{\lambda_\beta^2 - \gamma^2/256}{1+\gamma^2/256}\cdot\tau} \quad (22)$$

Condition (22) contains the pilot time delay τ that can drive the RPC.

Figure 8 shows the migration of the values of attitude gain K_ϕ at the stability boundary as a function of τ. It can be seen that increasing the time delay to 200ms results in a reduction of the available attitude feedback gain by 6% for Puma helicopter (instability at K_ϕ=0.945). It follows that the space for designing the FCS is somewhat limited, although the effect is not particularly strong.

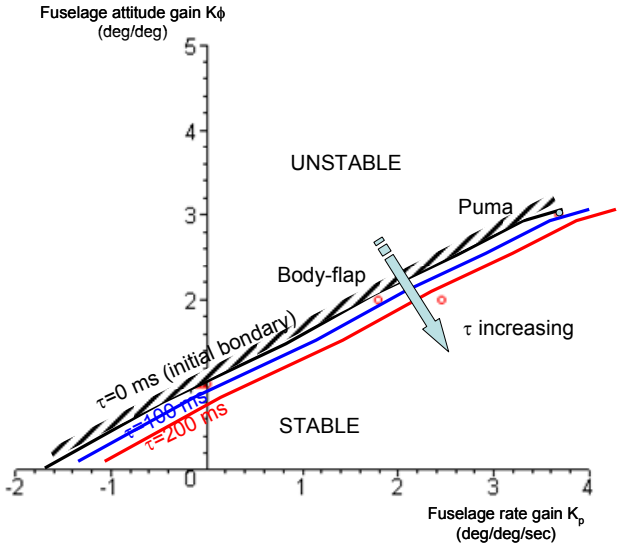

Figure 8: *Roll attitude feedback boundary as time delay is introduced in the pilot input*

These results will now be extended to include coupled flap-lag-roll motion.

The Mechanism of flap-lag-roll coupling in a Category I RPC

The energy flow method can also be applied to the flap-lag-roll equations of motion (11) - (13), when a time delay is included in the pilot input. First it is assumed that the roll motion is an "external" excitation for the flapping motion. Using a controller with gain K_ϕ, the roll motion pumps energy into the flap motion, and the flapping motion acts as an external excitation for the roll motion. It can be seen that the RPC event criterion (19) now takes the form:

$$\frac{1}{(\nu+1)^2(\nu-1)^2}\left[\begin{array}{l}\left(2-\tau\frac{\gamma}{8}K_\phi\right)\nu\left(\nu^2-1\right)\left(1+\cos 2\psi\right)+\\ \frac{\gamma}{8}\left(\nu\left(\nu^2-1\right)+K_\phi\left(\nu^2+1\right)\right)\sin 2\psi\end{array}\right]<0 \tag{23}$$

Rearranging the terms in the parenthesis of eq. (23) and identifying the sign of each term gives:

$$\underbrace{\frac{\gamma}{8}K_\phi}_{+}\left[\underbrace{\left(\nu^2+1\right)\sin 2\psi}_{+/-\ fct(\psi)}-\underbrace{\tau\left(\nu^2-1\right)\left(1+\cos 2\psi\right)}_{+}\right]+ \tag{24}$$
$$\underbrace{2\nu\left(\nu^2-1\right)+2\nu\left(\nu^2-1\right)\cos 2\psi+\frac{\gamma}{8}\nu\left(\nu^2-1\right)\sin 2\psi<0}_{+\ for\ \gamma\in[5,15]}$$

M_β now has the same sign as β', therefore the roll and flap motions mutually transfer energy into each other, destabilizing the system. This is especially true for helicopters with large rotor Lock numbers and for time delays higher than about 200ms. Figure 9 summarizes the energy flow transfer from the fuselage to the flap and back in a category I RPC event for a hovering helicopter.

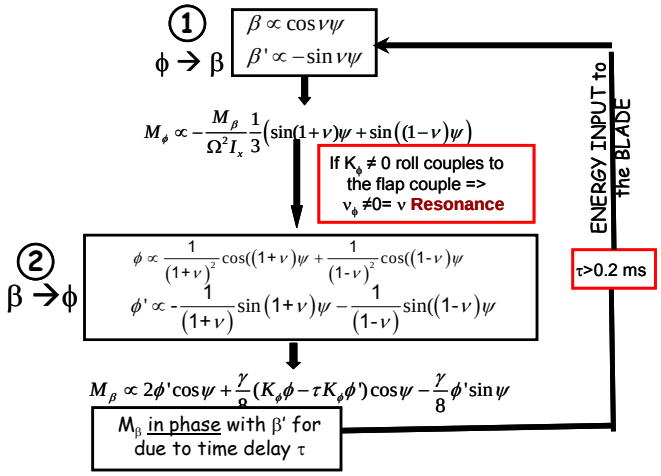

Figure 9: *The flap-roll mechanism in a PIO using the energy flow method*

Figure 10 shows the energy flow for the adverse RPC event. In this case, it can be seen that there is a vicious circle of energy transmission between the fuselage and flap motion which can be reinforced by the contribution of the lag mode to the instability. The energy flow method provides a system view on stability and can be extended to explore the specific contributions of rotor design parameters to stability boundaries. Moreover, active control mechanisms that divert the negative flow of energy offer potential solutions to what appears to be an all too common problem in modern helicopter design.

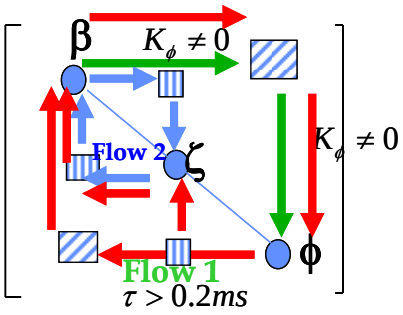

Figure 10: *The energy flow in the roll-flap-lag equations in a RPC*

Concluding Remarks

The study reported in this paper was undertaken to increase understanding of the mechanisms through which the pilot or FCS inputs can excite the higher-order flap-lag rotor motions. The investigation has concentrated on the body roll motion as it is generally much faster than the body pitch motion, and couples with the rotor motions in such a way that they impose limitations on the FCS feedback gains. The paper has presented an approximate analysis to explain the results that rate feedback can destabilize the rotor lagging motion and attitude feedback can destabilize the rotor flapping motion. Stiff-inplane, soft flapwise rotors are the most susceptible to instabilities involving body-flap-lag modes.

The energy flow process has been used to examine the mechanism through which the rotor motions pump energy into the fuselage roll mode; it was demonstrated that, in the case of a category I RPC event, the flap and roll motion mutually pump energy into each other, the lag mode contributing to the exchange of energy through the flap-lag coupling. Any additional time delay τ introduced by the pilot or digital artifacts in the FCSs will narrow the design space even

further in terms of the FCS gains. However, it appears that τ has not much influence on the limits of attitude controller. The approximate analysis can be used in design to evaluate the effectiveness of active rotor control on the stability boundaries.

References

1. anon, "Flight Control Design – Best Practices", RTO-TR-029, RTO/NATO report, Dec. 2000
2. Bielawa, Richard L., "Rotary Wing Structural Dynamics and Aeroelasticity", AIAA Education Series, 1992
3. Curtiss, H.C., Jr., "Stability and Control Modelling", VERTICA, Vol.12, No.4, pp 381-394, 1988
4. Curtiss, H.C., Jr., "Physical Aspects of Rotor Body Coupling in Stability and Control", "46th AHS Forum Proceedings, Washington DC, May 1990
5. Dryfoos, James, Mayo, John, Kothmann, Bruce, "An Approach to Reducing Rotor-Body Coupled Roll Oscillations on the RAH-66 Comanche using Modified Roll Rate Feedback", 55th AHS Forum Proceedings, Montreal, Canada, May 1999
6. Hamel, Peter G., "Rotorcraft –Pilot Couplings. A Critical Issue for Highly Augmented Helicopters?", Paper presented at the FVP Symposium an Advances in Rotorcraft Technology, Ottawa, Canada, 27-30 May 1996, AGARD CP-592
7. Hohenemser, K., "Hingeless Rotorcraft Flight Mechanics", AGARD-AG-197, 1974
8. Holten, Th. van, "Energy Flow Considerations, an Educational Tool to Clarify Aeroelastic Phenomena", 26th European Rotorcraft Forum, September 26-29, 2000, The Hague, The Netherlands
9. Johnson, Wayne, "Helicopter Theory", Dover Publications, 1980
10. Klyde, David H., Mitchell, David G., "A PIO Case Study – Lessons Learned through Analysis", AIAA Atmospheric Flight Mechanics Conference and Exhibit, San Francisco, August 15-18, 2005
11. McKay, K., (1994), "Pilot Induced Oscillation – A Report on the AGARD Workshop on PIO, 13th May, 1994", AGARD CP-560
12. McRuer, D.T., et al., (1997), "Aviation Safety and Pilot Control. Understanding and Preventing Unfavorable Pilot-Vehicle Interactions", ASEB National Research Council, National Academy Press, Washington D.C., 1997
13. Mitchell, David G., et. al., "Evolution, Revolution and Challenges of Handling Qualities", J. of Guidance, Control and Dynamics, Vol. 27, No.1, Jan-Feb. 2004, pp. 12-28
14. Padfield, Gareth D., "Helicopter Flight Dynamics", (second edition) Blackwell Science, 2007
15. Pavel, Marilena D., "Quantification of the Flap-Lag Coupling for a Helicopter Rotor Blade in Hovering Flight", International Forum on Aeroelasticity and Structural Dynamics (IFASD), 18-20 June 2007, Stockholm, Sweden
16. Strehlow, H, Presentation of Eurocopter Germany for the "GARTEUR HC Exploratory Group (EG-22) On Pilot Activated Oscillations/ Rotorcraft Pilot Coupling", Nov. 2003
17. Walden, R. Barry, "A Retrospective Survey of Pilot-Structural Coupling Instabilities Naval Rotorcraft", 63rd Annual Forum of the American Helicopter Society, Virginia Beach, VA May 1-3, 2007

Appendix A: Derivation of Roll-Flap Equations of Motion in Matrix Form

The system of equations (1) can be written in matrix form as:

$$\begin{bmatrix} \beta_{1c}' \\ \beta_{1s}' \\ \overline{q}' \\ \overline{p}' \end{bmatrix} = A_{RF} \begin{bmatrix} \beta_{1c} \\ \beta_{1s} \\ \overline{q} \\ \overline{p} \end{bmatrix} + B_{RF} \begin{bmatrix} \theta_{1s} \\ \theta_{1c} \end{bmatrix} \qquad \text{(A1)}$$

where the matrices A and B are given by:

$$A_{RF} = \begin{bmatrix} -8\frac{\gamma\left(-3+\lambda_\beta{}^2\right)}{-256+\gamma^2} & -\frac{128\lambda_\beta{}^2-128+\gamma^2}{-256+\gamma^2} & 1 & 32\frac{\gamma}{-256+\gamma^2} \\ \frac{-128\lambda_\beta{}^2+128+\gamma^2}{-256+\gamma^2} & -8\frac{\gamma\left(1+\lambda_\beta{}^2\right)}{-256+\gamma^2} & 0 & \frac{256+\gamma^2}{-256+\gamma^2} \\ -\frac{M_\beta}{I_y\Omega^2} & 0 & 0 & 0 \\ 0 & -\frac{M_\beta}{I_x\Omega^2} & 0 & 0 \end{bmatrix} \qquad \text{(A2)}$$

$$B_{RF} = \begin{bmatrix} 16\dfrac{\gamma}{-256+\gamma^2} & \dfrac{\gamma^2}{-256+\gamma^2} \\ \dfrac{\gamma^2}{-256+\gamma^2} & 16\dfrac{\gamma}{-256+\gamma^2} \\ 0 & 0 \\ 0 & 0 \end{bmatrix} \quad \text{(A3)}$$

Assuming a controller $\theta_{1c} = K_\phi \phi, \quad K_\phi > 0$, transforms system (A1) into a fifth-order coupled system of the form:

$$\begin{bmatrix} \beta_{1c}' \\ \beta_{1s}' \\ q' \\ p' \\ \phi' \end{bmatrix} = A_{RF}^{*} \begin{bmatrix} \beta_{1c} \\ \beta_{1s} \\ q \\ p \\ \phi \end{bmatrix} + B_{RF}^{*} \theta_{1s} \quad \text{(A4)}$$

where the matrices A and B are given by:

$$A_{RF}^{*} = \begin{bmatrix} -8\dfrac{\gamma\left(-3+\lambda_\beta^{\,2}\right)}{-256+\gamma^2} & -\dfrac{128\lambda_\beta^{\,2}-128+\gamma^2}{-256+\gamma^2} & 1 & 32\dfrac{\gamma}{-256+\gamma^2} & -\dfrac{\gamma^2 K_\phi}{-256+\gamma^2} \\ \dfrac{-128\lambda_\beta^{\,2}+128+\gamma^2}{-256+\gamma^2} & -8\dfrac{\gamma\left(1+\lambda_\beta^{\,2}\right)}{-256+\gamma^2} & 0 & \dfrac{256+\gamma^2}{-256+\gamma^2} & -16\dfrac{\gamma K_\phi}{-256+\gamma^2} \\ -\dfrac{M_\beta}{I_y\Omega^2} & 0 & 0 & 0 & 0 \\ 0 & -\dfrac{M_\beta}{I_x\Omega^2} & 0 & 0 & 0 \\ 0 & 0 & 0 & 1 & 0 \end{bmatrix} \quad \text{(A5)}$$

$$B_{RF}^{*} = \begin{bmatrix} 16\dfrac{\gamma}{-256+\gamma^2} \\ \dfrac{\gamma^2}{-256+\gamma^2} \\ 0 \\ 0 \\ 0 \end{bmatrix} \quad \text{(A6)}$$

For high values of feedback gain one can make the assumption that the coupled roll regressing flap mode and roll subsidence mode define a high modulus system. This leads to a 4th order system of equations in $\{\beta_{1s}, \beta_{1c}, p, \phi\}$:

$$\begin{bmatrix} \beta_{1c}' \\ \beta_{1s}' \\ p' \\ \phi' \end{bmatrix} = A_{RF}^{**} \begin{bmatrix} \beta_{1c} \\ \beta_{1s} \\ p \\ \phi \end{bmatrix} + B_{RF}^{**} \theta_{1s} \quad \text{(A7)}$$

with A and B given by:

$$A_{RF}^{**} = \begin{bmatrix} -8\dfrac{\gamma\left(-3+\lambda_\beta^{\,2}\right)}{-256+\gamma^2} & -\dfrac{128\lambda_\beta^{\,2}-128+\gamma^2}{-256+\gamma^2} & 32\dfrac{\gamma}{-256+\gamma^2} & -\dfrac{\gamma^2 K_\phi}{-256+\gamma^2} \\ \dfrac{-128\lambda_\beta^{\,2}+128+\gamma^2}{-256+\gamma^2} & -8\dfrac{\gamma\left(1+\lambda_\beta^{\,2}\right)}{-256+\gamma^2} & \dfrac{256+\gamma^2}{-256+\gamma^2} & -16\dfrac{\gamma K_\phi}{-256+\gamma^2} \\ 0 & -\dfrac{M_\beta}{I_x\Omega^2} & 0 & 0 \\ 0 & 0 & 1 & 0 \end{bmatrix} \quad \text{(A8)}$$

$$B_{RF}^{**} = \begin{bmatrix} 16\dfrac{\gamma}{-256+\gamma^2} \\ \dfrac{\gamma^2}{-256+\gamma^2} \\ 0 \\ 0 \end{bmatrix} \quad \text{(A9)}$$

The characteristic equation of system (A7) represents a fourth-order equation of the form:

$$a_4\lambda^4 + a_3\lambda^3 + a_2\lambda^2 + a_1\lambda^1 + a_0 = 0 \quad \text{(A10)}$$

The coefficients of the characteristic equation are:

$$\begin{aligned} a_4 &= 1 \\ a_3 &= 16\frac{\gamma\left(\lambda_\beta^2 - 1\right)}{-256+\gamma^2} \\ a_2 &= \frac{\Omega^2\gamma^2 - 128\Omega^2\lambda_\beta^2 + 64\Omega^2\lambda_\beta^4 + 64\Omega^2}{\Omega^2\left(-256+\gamma^2\right)} + \frac{M_\beta\left(256+\gamma^2\right)}{I_x\Omega^2\left(-256+\gamma^2\right)} \\ a_1 &= -8\frac{\gamma M_\beta\left(2K_\phi - 1 - \lambda_\beta^2\right)}{I_x\Omega^2\left(-256+\gamma^2\right)} \\ a_0 &= -\frac{\gamma^2 M_\beta K_\phi}{I_x\Omega^2\left(-256+\gamma^2\right)} \end{aligned} \quad \text{(A11)}$$

Appendix B: Flap-Lag Equations in Energy Flow Method

We start from the flap-lag equations of motion in hovering case, which in the rotating frame are given by:

$$\beta'' + \frac{\gamma}{8}\beta' + \left(1+\nu_\beta^{\,2}\right)\beta + 2\beta_0\nu_\beta^{\,2}\zeta' = 0$$
$$\zeta'' + \nu_\zeta^{\,2}\zeta + \left(\nu_\beta^{\,2}-1\right)\beta_0\beta' = 0 \qquad \text{(B1)}$$

with $\lambda_\beta^2 = 1 + \frac{K_\beta}{I_\beta\Omega^2} = 1+\nu_\beta^2$ the non-dimensional flap frequency and $\lambda_\zeta^2 = \nu_\zeta^2 = \frac{K_\zeta}{I_{bl}\Omega^2}$ the non-dimensional lead-lag frequency. Assuming now that one degree of freedom is excitation for the other, (B1) can be written as:

$$\beta'' + \frac{\gamma}{8}\beta' + \left(1+\nu_\beta^{\,2}\right)\beta = -2\beta_0\nu_\beta^{\,2}\zeta' = M_\beta$$
$$\zeta'' + \nu_\zeta^{\,2}\zeta = -\left(\nu_\beta^{\,2}-1\right)\beta_0\beta' = M_\zeta \qquad \text{(B2)}$$

Consider first that the lagging motion is an "external" excitation for the flapping. Assume that all the natural frequencies coincide $\lambda_\beta = \nu_\zeta = \nu$ and also that the resulting flapping oscillation is proportional to $\cos\nu\psi$, i.e. $\beta \propto \cos\nu\psi$. The flap velocity is then proportional to $\beta' \propto -\sin\nu\psi$.

The excitation M_ζ of the lagging degree of freedom is thus proportional with,

$$M_\zeta \propto -\left(\nu_\beta^{\,2}-1\right)\beta_0(-\sin\nu\psi) = \left(\nu_\beta^{\,2}-1\right)\beta_0\sin\nu\psi \qquad \text{(B3)}$$

The response of the lead-lag motion is given by the solution to the equation $\zeta'' + \nu_\zeta^{\,2}\zeta = M_\zeta$. Because the excitation contains terms which have the same frequency as the frequency of the system ($\nu_\beta \approx \nu_\zeta \approx \nu$) it follows that the system is at resonance, so the lead-lag response is 90 deg out of phase with the external excitation. This means that the lead-lag response will be proportional to:

$$\zeta \propto -\left(\nu_\beta^{\,2}-1\right)\beta_0\sin(\nu\psi+90) \propto -\left(\nu_\beta^{\,2}-1\right)\beta_0\cos\nu\psi \qquad \text{(B4)}$$

Therefore the lagging velocity is proportional to $\zeta' \propto \left(\nu_\beta^{\,2}-1\right)\beta_0\sin\nu\psi$. It is known that a harmonic force acting on a vibrating system of the same frequency produces work on the system if the force is in phase with the velocity of the vibration. If so, the coupling term which represents this excitation pumps energy into the degree of freedom. For the flap-lag case, this means that the lagging velocity must contain terms that are in phase with the excitation (B4). This is true only when $\left(\nu_\beta^{\,2}-1\right) < 0$, i.e. $\nu_\beta^{\,2} < 1$. Therefore, the lead-lag due to flapping pumps energy into the lead-lag motion if $\nu_\beta^{\,2} < 1$.

Next, consider that the flapping motion acts as an external excitation for the lagging motion. The response of the lag angle is given by (B4). This causes in turn an external excitation of the flapping motion proportional to:

$$M_\beta \propto -2\beta_0\nu_\beta^{\,2}\zeta' \propto 2\beta^2{}_0\nu_\beta^{\,2}\left(\nu_\beta^{\,2}-1\right)\sin\nu\psi \qquad \text{(B5)}$$

The response of the flapping angle is given by the equation $\beta'' + \frac{\gamma}{8}\beta' + \left(1+\nu_\beta^{\,2}\right)\beta = M_\beta$. It follows that M_β, eq. (B5), is in or out of phase with the flap velocity $\beta' \propto -\sin\nu\psi$ depending on the sign of $\left(\nu_\beta^{\,2}-1\right)$. If $0 < \nu_\beta^{\,2} < 1$, then the flapping excitation due to lagging M_β contains a term which is in phase with the flapping velocity, so the lead-lag pumps energy into the flap. This corresponds to a soft-flapwise rotor according to ref. 7. Figure 11 describes these explanations. This result agrees with the classical theory of flap-lag instability [ref. 9] which demonstrates that the most critical flap-lag coupling corresponds to the case of $1 < \lambda_\beta < 1.15$ i.e. a soft flapwise rotor.

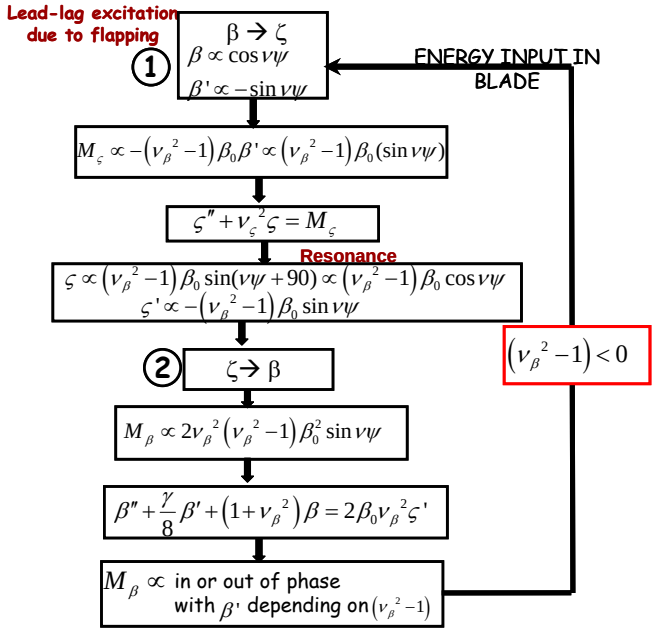

Figure 11 *The flap-lag mechanism of instability*

Looking back at the origin of the term $\left(\nu_\beta^{\,2}-1\right)\beta_0\beta'$, one sees that this corresponds to the Coriolis force on the blade due to a flapping velocity and represents the most critical parameter allowing transfer of energy.